

---

# On the Local Hessian in Back-propagation

---

**Huishuai Zhang**  
Microsoft Research Asia  
Beijing, 100080  
huzhang@microsoft.com

**Wei Chen**  
Microsoft Research Asia  
Beijing, 100080  
wche@microsoft.com

**Tie-Yan Liu**  
Microsoft Research Asia  
Beijing, 100080  
tyliu@microsoft.com

## Abstract

Back-propagation (BP) is the foundation for successfully training deep neural networks. However, BP sometimes has difficulties in propagating a learning signal deep enough effectively, e.g., the vanishing gradient phenomenon. Meanwhile, BP often works well when combining with “designing tricks” like orthogonal initialization, batch normalization and skip connection. There is no clear understanding on what is essential to the efficiency of BP. In this paper, we take one step towards clarifying this problem. We view BP as a solution of *back-matching propagation* which minimizes a sequence of back-matching losses each corresponding to one block of the network. We study the Hessian of the local back-matching loss (*local Hessian*) and connect it to the efficiency of BP. It turns out that those designing tricks facilitate BP by improving the spectrum of local Hessian. In addition, we can utilize the local Hessian to balance the training pace of each block and design new training algorithms. Based on a scalar approximation of local Hessian, we propose a scale-amended SGD algorithm. We apply it to train neural networks with batch normalization, and achieve favorable results over vanilla SGD. This corroborates the importance of local Hessian from another side.

## 1 Introduction

Deep neural networks have been advancing the state-of-the-art performance over a number of tasks in artificial intelligence, from speech recognition [Hinton et al., 2012], computer vision [He et al., 2016a] to natural language understanding [Hochreiter and Schmidhuber, 1997]. These problems are typically formulated as minimizing non-convex objectives parameterized by the neural network models. Typically, the models are trained with stochastic gradient descent (SGD) or its variants and the gradient information is computed through back-propagation (BP) [Rumelhart et al., 1986].

It is known that BP sometimes has difficulties in propagating a learning signal deep enough effectively, e.g., the *vanishing/exploding gradient phenomenon*, [Hochreiter, 1991, Hochreiter et al., 2001]. Recent designing tricks, such as orthogonal initialization [Saxe et al., 2014], batch normalization [Ioffe and Szegedy, 2015] and skip connection [He et al., 2016a], improve the performance of deep neural networks on almost all tasks, which are interpreted to be able to alleviate the vanishing gradient to some extent. However, a recent work [Orhan and Pitkow, 2018] shows that a network with non-orthogonal skip connection always underperforms a network with orthogonal (identity is a special case) skip connection and neither network has vanishing gradient as back-propagating through layers. This suggests that vanishing gradient is not the core reason for a network being good or not. We ask that *if vanishing gradient is a superficial reason, what is essential to the efficiency of BP?*

In this paper, we consider this question from the optimization’s perspective and give an answer: the Hessian of the local back-matching loss is responsible for the difficulty of training deep nets with BP. Specifically, we start from a penalized loss formulation, which takes the intermediate feature outputs as variables of the optimization and the penalty is to enforce the coordination (architecture) connection [Carreira-Perpinan and Wang, 2014]. Minimizing the penalized loss following backward

order leads to a *back-matching propagation* procedure which involves minimizing a sequence of back-matching losses. Each back-matching loss penalizes the mismatch between a target signal from the upper block and the output of the current block, which is determined by the parameters and the inputs of the block<sup>1</sup>. We show that BP is equivalent to minimizing each back-matching loss with one-step gradient update. This is to say, BP is a solution of the back-matching propagation procedure.

However, in general, the one-step gradient update may/may not be a good solution to minimize the back-matching loss contingent on the Hessian, as is well known that bad-conditioned Hessian can have enormous adversarial impact on the convergence of the first-order methods [Ben-Tal and Nemirovski, 2001]. Loosely speaking, if the local Hessian is badly-conditioned, the one-step gradient update does not minimize the back-matching loss sufficiently and the target signal distorts gradually when backward through layers.

We mathematically derive the formula of local Hessian and show that the designing tricks including batch normalization and skip connection can drive local Hessian towards a good-conditioned matrix to some extent. This explains why practical designing tricks can stabilize the backward process. In particular, by analyzing the local Hessian of residual block, we can answer the questions about skip connection in [Orhan and Pitkow, 2018] via local Hessian.

Besides interpreting existing practical techniques and providing guidance to design neural network structure, we can also utilize local Hessian to design new algorithms. The general idea is to employ the information of the local Hessian to facilitate the training of neural networks. We propose a scale-amended SGD algorithm to balance the training pace of each block by considering the scaling effect of local Hessian. More specifically, we approximate the local Hessian with a scalar and use the scalar to amend the gradient of each block. Such a scale-amended SGD is built upon the regular BP process, and hence it is easy to implement in current deep learning frameworks [Bastien et al., 2012, Abadi et al., 2016, Paszke et al., 2017, Seide and Agarwal, 2016]. We apply this scale-amended SGD to feed-forward networks with batch normalization and empirically demonstrate that it improves the performance by a considerable margin. This further advocates the key role of the local Hessian in efficient learning of deep neural networks.

## 1.1 Related Works

The penalty loss formulation is inspired by *methods of auxiliary coordinates (MAC)* [Carreira-Perpinan and Wang, 2014] and *proximal backpropagation* [Frerix et al., 2018]. Specifically, Carreira-Perpinan and Wang [2014] applies block coordinate descent to optimize the penalized objective. Frerix et al. [2018] applies proximal gradient when updating  $W$ . In contrast, we start from the penalty loss formulation and focus on the local Hessian for each subproblem in the back-matching propagation, and argue that the local Hessian is critical to the efficiency of BP.

Our scale-amended SGD is related to the algorithms tackling the difficulty of BP for training deep nets by incorporating second-order/metric information [Martens, 2010, Amari, 1998, Pascanu and Bengio, 2014, Ollivier, 2015, Martens and Grosse, 2015] and the block-diagonal second order algorithms [Lafond et al., 2017, Zhang et al., 2017, Grosse and Martens, 2016]. These second-order algorithms approximate the Hessian/Fisher matrix and are computationally expensive. In contrast, the scale-amended SGD only amends the vanilla SGD with a scalar for each block based on the approximation of local Hessian. The scale-amended SGD is closely related to the layer-wise adaptive learning rate strategy [Singh et al., 2015, You et al., 2017]. However, these two layer-wise learning rate strategies do not have explanation of why the rate is set in that way.

## 2 BP as a solution of back-matching propagation

In this section, we first introduce the quadratic penalty formulation of the loss of neural network and the *back-matching propagation* procedure which minimizes a sequence of local back-matching losses following the backward order. Then we connect BP to the one-step gradient update solution of back-matching propagation procedure. The quality of such a solution on minimizing back-matching loss is determined by its local Hessian.

---

<sup>1</sup>Here a block can be composed of one layer or multiple layers.

---

**Procedure 1** Back-matching Propagation

---

**Input:**  $\mathbf{W}_b^k, \mathbf{z}_b^k$  for  $b = 1, \dots, B$  and  $\mathbf{z}_0^k = X^k$ .

**for**  $b = B, \dots, 1$  **do**

$$\mathbf{W}_b^{k+1} \leftarrow \arg \min_{\mathbf{W}_b} \ell_b(\mathbf{W}_b, \mathbf{z}_{b-1}^k), \quad (3)$$

$$\mathbf{z}_{b-1}^{k+\frac{1}{2}} \leftarrow \arg \min_{\mathbf{z}_{b-1}} \ell_b(\mathbf{W}_b^k, \mathbf{z}_{b-1}), \quad (4)$$

**end for**

**Output:** A new parameter  $\mathbf{W}^{k+1}$

---

Suppose the loss of training a neural network is given by<sup>2</sup>

$$J(\mathbf{W}; X, y) = \ell(y; F(\mathbf{W}, X)), \quad (1)$$

where  $\ell(\cdot)$  is the loss function with respect to the training targets  $y$  and the network output,  $F(\cdot, \cdot)$  is the network mapping,  $\mathbf{W}$  is the trainable parameter of the network and  $X$  is the input data. Carreira-Perpinan and Wang [2014] introduces the intermediate output of the network as auxiliary variables and the architecture connection as a quadratic penalty, and proposes to minimize the following quadratic penalty formulation of the loss,

$$Q(\mathbf{W}, \mathbf{z}; \gamma) = \ell(y, F_B(\mathbf{W}_B, \mathbf{z}_{B-1})) + \sum_{b=1}^{B-1} \frac{\gamma}{2} \|\mathbf{z}_b - F_b(\mathbf{W}_b; \mathbf{z}_{b-1})\|^2, \quad (2)$$

where  $F_b(\cdot, \cdot)$  is a block mapping,  $\mathbf{W}_b, \mathbf{z}_{b-1}$  are the trainable parameter and the input of network block  $b$ , respectively, for  $b = B, \dots, 1$  and  $\mathbf{z}_0$  is the input data  $X$ .

It has been argued in [Nocedal and Wright, 2006] that under mild condition, the solutions of minimizing (2) converge to the solution of the original problem (1) as  $\gamma \rightarrow \infty$ . Carreira-Perpinan and Wang [2014] minimizes objective (2) via  $z$ -step and  $W$ -step, which is essentially a block coordinate descent algorithm.

Inspired by the form (2), we study the back-matching propagation procedure (Procedure 1), which minimizes a sequence of local back-matching losses following the backward order. The local back-matching loss for block  $b$  at step  $k$  is denoted by  $\ell_b$

$$\ell_b(\mathbf{W}_b, \mathbf{z}_{b-1}) = \begin{cases} \ell(\mathbf{y}^k; F_B(\mathbf{W}_B, \mathbf{z}_{B-1})), & \text{for } b = B \\ \frac{1}{2} \left\| \mathbf{z}_b^{k+\frac{1}{2}} - F_b(\mathbf{W}_b, \mathbf{z}_{b-1}) \right\|^2, & \text{for } b = B-1, \dots, 1, \end{cases} \quad (5)$$

where  $\mathbf{z}_b^{k+\frac{1}{2}}$  is computed by (4) repeatedly. We note that  $\mathbf{z}^k$  is computed by forward pass given a new  $X^k$  and is not updated by Procedure 1 and  $\mathbf{z}_b^{k+\frac{1}{2}}$  is an intermediate variable to store the desired change on the output  $\mathbf{z}_b$  which is used to compute  $\mathbf{W}_{b-1}^{k+1}$ . For each subproblem at  $b$ , we alternatively optimize over  $\mathbf{W}_b$  and  $\mathbf{z}_{b-1}$  while fixing the other as in the forward process because jointly optimizing over  $\mathbf{W}_b$  and  $\mathbf{z}_{b-1}$  is non-convex even if  $F_b$  represents matrix-vector product.

A direct explanation of the back-matching loss is that given the target signal  $\mathbf{z}_b^{k+\frac{1}{2}}$  propagated from upper block, which is believed to be the direction of  $\mathbf{z}_b^k$  to decrease the loss, the new weight  $\mathbf{W}^{k+1}$  and the new target signal for lower block  $\mathbf{z}_{b-1}^{k+\frac{1}{2}}$  should minimize the matching loss  $\ell_b$ .

We are not suggesting Procedure 1 as a new algorithm to train neural network. Actually, Procedure 1 may not be stable in practice if solving each subproblem fully [Lee et al., 2015, Wiseman et al., 2017] because the solution of (3) and (4) may deviate from last updated value too much and jump out of the trust region. Instead, we connect BP to the one-step gradient update solution of (3) and (4) and argue that the conditions of the subproblems (3) and (4) affect the efficiency of BP given the explanation of back matching loss.

**Proposition 1.** *If (3) is solved by one-step gradient update with step size  $\mu$  and (4) is solved by one-step gradient update with step size 1, then  $\mathbf{W}^{k+1}$  produced by the procedure 1 is the same as gradient update of the original problem (1) with step size  $\mu$ .*

<sup>2</sup>For simplicity we omit the bias term in the sequel.

*Proof.* The proof is relegated to Supplemental A due to space limit.  $\square$

We note that the form of the back-matching loss is mentioned in *target propagation* [Lee et al., 2015, Le Cun, 1986] which is motivated by the biological implausibility of BP while we formulate it from minimizing a penalized objective. We also note that the connection between BP and the one-step gradient update of minimizing (2) in backward order is made in [Frerix et al., 2018] for the case  $F_b(\cdot)$  is either activation function or linear transformation.

Here we view BP as a solution of back-matching propagation and study the local Hessian matrices of back-matching losses (3) and (4),

$$\text{Local Hessian: } \mathbf{H}_{\text{vec}(\mathbf{W})} = \frac{\partial^2 \ell_b(\mathbf{W}_b, \mathbf{z}_{b-1}^k)}{\partial \text{vec}(\mathbf{W})^2}, \quad \mathbf{H}_z = \frac{\partial^2 \ell_b(\mathbf{W}_b^k, \mathbf{z}_{b-1})}{\partial \mathbf{z}_{b-1}^2}. \quad (6)$$

The Hessian of training deep neural networks has been studied in previous works Dauphin et al. [2014], Orhan and Pitkow [2018], Li et al. [2016], Sagun et al. [2017], Jastrzebski et al. [2018]. They all analyze and calculate the Hessian of the objective with respect to the whole network parameter. In contrast, we study the Hessian of the local back-matching loss and connect it to the efficiency of BP.

Loosely speaking, if the local Hessian of (5) with respect to  $\mathbf{W}$  is good-conditioned, the solution of (3) minimizes the local back-matching loss sufficiently, which implies that the target signal is efficiently approximated by updating parameters of current block, and if the local Hessian of (5) with respect to  $\mathbf{z}$  is good-conditioned, the solution of (4) minimizes the local back-matching loss sufficiently, which implies that the target signal is efficiently back-propagated. Next, we show how skip connection and batch normalization improve the spectrum of the local Hessian.

### 3 Explain the efficiency of BP via local Hessian

Because the condition of local Hessian determines how efficiently the back-matching loss is minimized by updating the parameters of current block and how accurately the error signal propagates back to the lower layer, we evaluate how good a block is via analyzing its local Hessian. We first analyze the local Hessian of a fully connected layer<sup>3</sup> and then show that the skip connection and batch normalization improve the spectrum of local Hessian and hence facilitate the efficiency of BP.

#### 3.1 Block of a fully connected layer

We consider a block  $b$  composed of a fully connected layer with  $n_b$  outputs and  $n_{b-1}$  inputs. The mapping function is given by

$$\mathbf{z}_b = F_b(\mathbf{W}_b, \mathbf{z}_{b-1}) = \mathbf{W}_b \cdot \mathbf{z}_{b-1}, \quad (7)$$

where  $\mathbf{W}_b$  is an  $n_b \times n_{b-1}$  matrix.

Suppose that after the gradient step on  $\mathbf{z}_b$  from upper layer, we get an intermediate variable  $\mathbf{z}_b^{k+1/2}$ . The Hessian of back matching loss (5) with respect to  $\mathbf{z}_{b-1}$  and  $\mathbf{w}_b$  are

$$\mathbf{H}_z = (\mathbf{W}_b^k)^T \mathbf{W}_b^k, \quad (8)$$

$$\mathbf{H}_w = \sum_{j=1}^m \mathbf{z}_{b-1}^k[j] (\mathbf{z}_{b-1}^k[j])^T, \quad (9)$$

respectively, where  $m$  is the batch size,  $[j]$  represents the  $j$ -th sample and  $\mathbf{w}_b$  is a vector of a row of  $\mathbf{W}_b$ . Then  $\mathbf{H}_{\text{vec}(\mathbf{W}_b)}$  is a block diagonal matrix with each block being  $\mathbf{H}_w$  where  $\text{vec}(\mathbf{W}_b)$  is a long vector stacking the rows of  $\mathbf{W}_b$  first.

For (8) the local Hessian with respect to  $\mathbf{z}_{b-1}$ , we derive the distribution of its eigenvalues. For the convenience of analysis, we assume the elements of  $\mathbf{w}_b$  are independently generated from Gaussian distribution with mean 0 and variance  $\sigma^2$  and  $n_b, n_{b-1} \rightarrow \infty$  and the ratio  $n_b/n_{b-1} \rightarrow c \in (0, +\infty)$ .

<sup>3</sup>The formula for convolution layer is given in Supplemental C.

Then by the Marchenko-Pastur law [Marčenko and Pastur, 1967], we have the density of the eigenvalue  $\lambda$  of (8) as follows,

$$\nu(A) = \begin{cases} (1-c)\mathbf{1}_{0 \in A} + \nu_2(A), & \text{if } 0 < c \leq 1, \\ \nu_2(A), & \text{if } c > 1, \end{cases} \quad (10)$$

where

$$d\nu_2(\lambda) = \frac{c}{2\pi\sigma^2} \frac{\sqrt{(c_+ - \lambda)(\lambda - c_-)}}{\lambda} \mathbf{1}_{[c_-, c_+]} d\lambda, \quad (11)$$

with  $c_+ = \sigma^2(1 + \sqrt{c})^2/c$ ,  $c_- = \sigma^2(1 - \sqrt{c})^2/c$ .

This result affirms that the orthonormal initialization [Mishkin and Matas, 2016, Saxe et al., 2014] facilitates backward propagation. If  $\mathbf{W}_b$  is an orthonormal matrix, the eigenvalues of  $\mathbf{H}_z$  are composed of  $n_b$  1's and  $n_{b-1} - n_b$  0's if  $n_b < n_{b-1}$ . This is the best spectrum of Hessian we can expect for minimizing the back-matching loss (5).

However, in general,  $\mathbf{W}_b$  is not orthonormal and hence  $\mathbf{H}_z$  is not identity. The gradient update on  $\mathbf{z}_{b-1}$  does not minimize the back-matching loss well. As back propagating to lower blocks, the update  $\mathbf{z}_{b-t}^{k+\frac{1}{2}} - \mathbf{z}_{b-t}^k$  gets far from the direction of minimizing the back-matching loss  $\ell_b$  for  $t = 1, 2, \dots, b$ . Such discrepancy becomes larger as the condition of  $\mathbf{H}_z$  of each block is bad and as the back-propagation goes deep.

For the local Hessian with respect to  $\mathbf{W}$ , it is hard to control in general. Several recent works [Frerix et al., 2018, Ye et al., 2017] suggest using forms involving  $\mathbf{H}_W$  to precondition vanilla SGD. We note that Le Cun et al. [1991] has also studied the spectrum of  $\mathbf{H}_w$  which gives a theoretical justification for the choice of centered input over biased state variables.

We next study the local Hessian of blocks with skip connection and batch normalization and show that these designing tricks can improve the spectrum of  $\mathbf{H}_z$  and  $\mathbf{H}_W$  to some extent and hence make the training deep neural networks easier.

### 3.2 Block with skip connection

Skip connection has been empirically demonstrated important to obtain state-of-the-art results [He et al., 2016a,b, Huang et al., 2017a], while its functionality has various interpretations. Veit et al. [2016] argue that residual network can be seen as an ensemble of shallow nets and avoids vanishing gradient problem by introducing short paths. Jastrzebski et al. [2018] suggest that residual block performs iterative refinement of features for higher layer while lower layers concentrate representation learning behavior. These works focus on the interpretation of how Resnet works. We here try to give an answer on why Resnet works from the optimization perspective. A recent work [Orhan and Pitkow, 2018] argues that skip connection eliminates singular points of the Hessian matrix and there are open questions in [Orhan and Pitkow, 2018], for which we can give answers by analyzing the local Hessian of residual block.

Suppose that the mapping of residual block is given by

$$\mathbf{z}_b = F_b(\mathbf{W}_b, \mathbf{z}_{b-1}) = \mathbf{z}_{b-1} + \phi_b(\mathbf{W}_b, \mathbf{z}_{b-1}), \quad (12)$$

where  $F_b(\cdot)$  is the residual block mapping with parameters  $\mathbf{W}_b$  and input  $\mathbf{z}_{b-1}$ . The Hessians of the back-matching loss (5) with respect to  $\mathbf{z}_{b-1}$  and  $\mathbf{W}_b$  are given by

$$\mathbf{H}_z = \left( \mathbf{I} + \frac{\partial \phi_b}{\partial \mathbf{z}_{b-1}} \right)^T \left( \mathbf{I} + \frac{\partial \phi_b}{\partial \mathbf{z}_{b-1}} \right) - \frac{\partial}{\partial \mathbf{z}_{b-1}} \left( \frac{\partial F_b}{\partial \mathbf{z}_{b-1}} \cdot \left( \mathbf{z}_b^{k+\frac{1}{2}} - \mathbf{z}_b^k \right) \right), \quad (13)$$

$$\mathbf{H}_W = \left( \frac{\partial F_b}{\partial \text{vec}(\mathbf{W}_b)} \right)^T \left( \frac{\partial F_b}{\partial \text{vec}(\mathbf{W}_b)} \right) - \frac{\partial}{\partial \text{vec}(\mathbf{W}_b)} \left( \frac{\partial F_b}{\partial \text{vec}(\mathbf{W}_b)} \cdot \left( \mathbf{z}_b^{k+\frac{1}{2}} - \mathbf{z}_b^k \right) \right) \quad (14)$$

We can see that (14) the Hessian of local matching loss for residual block with respect to  $\mathbf{W}_b$  is the same as the case without skip connection. Thus we focus on (13) the local Hessian with respect to  $\mathbf{z}$ . Specifically, we analyze the first part of (13), the Gauss-Newton matrix, which is a good positive semidefinite approximation to the Hessian [Martens, 2016, Chen, 2011]. Define the condition number of a matrix  $\mathbf{M}$  as  $C(\mathbf{M}) := \sigma_{\max}(\mathbf{M})/\sigma_{\min}(\mathbf{M})$ , where  $\sigma_{\max}$  and  $\sigma_{\min}$  are the largest and smallest non-zero singular values, respectively. The larger the condition number, the worse the problem.

**Remark 1.** If **a)**  $\frac{\partial \phi_b}{\partial \mathbf{z}_{b-1}}$  is “small” relatively i.e.,  $\sigma_{\max} \left( \frac{\partial \phi_b}{\partial \mathbf{z}_{b-1}} \right) < 1 - s$  for some constant  $s > 0$ , and **b)**  $C \left( \frac{\partial \phi_b}{\partial \mathbf{z}_{b-1}} \right) > \frac{1+s}{1-s}$ , then

$$C \left( \mathbf{I} + \frac{\partial \phi_b}{\partial \mathbf{z}_{b-1}} \right) < C \left( \frac{\partial \phi_b}{\partial \mathbf{z}_{b-1}} \right). \quad (15)$$

This indicates that the condition number of the Gauss-Newton matrix with skip connection is guaranteed to be smaller than that without skip connection given two assumptions. The assumption **b)** is generally satisfied for neural network from the spectrum distribution analysis of fully-connected layer in Section 3.1 while the assumption **a)** seems a bit strong. We cannot verify assumption **a)** analytically because  $\phi_b(\cdot)$  typically involves more than two linear layers, nonlinear activations and batch normalization layers. We leave the empirical study on the spectrum distribution of local Hessian of the residual block for future work.

Interestingly, Orhan and Pitkow [2018] demonstrate that a network with an orthogonal connection achieves the performance as good as the one with identity skip connection, which can be easily explained from the fact that orthogonal skip connection does not change the condition number of the local Gauss-Newton matrix (the first part of (13)). Furthermore, Orhan and Pitkow [2018] also empirically show that a network with non-orthogonal skip connection always underperforms a network with orthogonal (identity is a special case) skip connection though neither network has vanishing gradient as back-propagating through layers. This can be easily argued from the formula (13) as non-orthogonal skip connection has larger condition number than orthogonal skip connection whose eigenvalues are all 1’s.

### 3.3 Block with batch normalization

Batch normalization (BN) is widely used for accelerating the training of feed-forward neural networks. In this section, we consider adding a BN layer after a fully-connected layer. We fix the affine transformation of BN to be identity for simplicity. If  $z_b^k$  represents one component of  $\mathbf{z}_b^k$  and  $\mathbf{w}_b$  a vector of one row of  $\mathbf{W}_b$ , then the BN layer mapping is given by

$$\tilde{z}_b^k = \text{BN}(\tilde{z}_b^k) = (\tilde{z}_b^k - \mathbb{E}[\tilde{z}_b^k]) / \sqrt{\text{Var}[\tilde{z}_b^k]}, \quad \text{where} \quad \tilde{z}_b^k = (\mathbf{w}_b)^T \mathbf{z}_{b-1}. \quad (16)$$

BP through a fully connected layer with BN is given in [Ioffe and Szegedy, 2015] and we provide the form for the back matching loss in Supplemental B for completeness. The gradient formula is quite complicated, as the  $\mathbb{E}$  and  $\text{Var}$  involve batch information. To proceed the analysis, we ignore the terms involving  $1/m$ , which does not lose much as the batch size becomes large.

Now we compute the local Hessian of the fully connected layer with BN as follows<sup>4</sup>

$$\mathbf{H}_z \approx \sum_{i=1}^{n_b} \frac{\mathbf{w}_b^k(i) \cdot \mathbf{w}_b^k(i)^T}{\text{Var}[\tilde{z}_b^k(i)]} = \sum_{i=1}^{n_b} \frac{\mathbf{w}_b^k(i) \cdot \mathbf{w}_b^k(i)^T}{\text{Var}[\mathbf{w}_b^k(i)^T \mathbf{z}_{b-1}^k]}, \quad (17)$$

$$\mathbf{H}_w \approx \frac{\sum_{j=1}^m \mathbf{z}_{b-1}^k[j] (\mathbf{z}_{b-1}^k[j])^T}{\text{Var}[\tilde{z}_b^k(i)]} = \frac{\sum_{j=1}^m \mathbf{z}_{b-1}^k[j] (\mathbf{z}_{b-1}^k[j])^T}{\text{Var}[\mathbf{w}_b^k(i)^T \mathbf{z}_{b-1}^k]}, \quad (18)$$

where  $n_b$  is the number of outputs of layer  $b$ ,  $\mathbf{w}_b^k(i)$  is the vector of the  $i$ -th row of  $\mathbf{W}_b^k$ , and  $\mathbf{z}_{b-1}^k[j]$  represents the input of the block  $b$  of the sample  $j$ . We next show how BN facilitates BP for training deep networks.

We first derive the distribution of the eigenvalues of (17) and compare it to (10) (the case without BN). Our assumption on  $\mathbf{w}_b$  is the same as the one to derive (11). In contrast to that  $\mathbf{H}_z$  being the sum of outer products of Gaussian vectors in Section 3.1, here  $\mathbf{H}_z$  is the sum of the outer products of  $\mathbf{w}_b / \|\mathbf{w}_b\|$ ’s which are the unit vectors equally distributed on the sphere. The density of the eigenvalue  $\lambda$  of (17) is of the form (10) with [Marčenko and Pastur, 1967],

$$d\nu_2(\lambda) = \frac{\sqrt{(c_+ - \lambda)(\lambda - c_-)}}{2\pi\lambda} \mathbf{1}_{[c_-, c_+]} d\lambda, \quad (19)$$

where  $c_+ = (1 + \sqrt{c})^2$ ,  $c_- = (1 - \sqrt{c})^2$ .

<sup>4</sup>We ignore the terms involving  $1/m$  again.

**Remark 2.** *Scaling the variance of the block parameter does not affect the spectrum of  $\mathbf{H}_z$  in (17).*

This is in contrast to (8) where the spectrum is linearly scaled with the variance of weight parameters. Thus BP gains benefit because it acts as one-step gradient update with fixed step size 1 for all blocks.

Another benefit of BN is to improve the condition of  $\mathbf{H}_w$  if  $\mathbf{z}_{b-1}$  is the output of a BN.

**Remark 3.** *If  $\mathbf{z}_{b-1}$  is the output of BN and  $\mathbf{w}_b$  is independent of  $\mathbf{z}_{b-1}$ , then  $\mathbb{E}\text{diag}(\mathbf{H}_w) = \mathbf{I}/\|\mathbf{w}_b\|^2$ .*

This indicates the problem (3) is well-conditioned and hence large step size is allowed [Ioffe and Szegedy, 2015].

## 4 Utilize local Hessian: An example

As previous section has shown the importance of the local Hessian, this section discuss how to utilize local Hessian to improve the performance on current deep learning tasks. One direct way of using local Hessian is to design better architecture. The spectrum of local Hessian can be a criteria to determine whether a building block is good or not for BP. One potential usage of local Hessian could be in neural architecture search [Zoph and Le, 2016]. As most of the time in neural architecture search is used to train huge amount of small networks and it will greatly accelerate if using local Hessian to prune the search space.

Another direction is to utilize the local Hessian to design new algorithms to improve the training of existing neural networks. Several works can be understood as examples, e.g., proximal propagation [Frerix et al., 2018] and Riemannian approaches [Cho and Lee, 2017, Huang et al., 2017b].

In this section, we propose a way to employ the information of the local Hessian to facilitate the training of deep neural networks. Ideally, good alternatives to minimize back-matching loss  $\ell_b$  are  $\mathbf{H}_W^{-1}\delta\mathbf{w}_b$  and  $\mathbf{H}_z^{-1}\delta\mathbf{z}_{b-1}$ , where  $\delta\mathbf{w}_b$  and  $\delta\mathbf{z}_{b-1}$  are the gradient computed via BP rule given  $\mathbf{z}^{k+\frac{1}{2}} - \mathbf{z}^k$ . However,  $\mathbf{H}_W$  and  $\mathbf{H}_z$  are often indefinite and expensive to compute. We suggest using two scalars  $m_{b,W}$  and  $m_{b,z}$  to evaluate how  $\mathbf{H}_W$  and  $\mathbf{H}_z$  scale the norm of a vector with general position, respectively. Then the back-matching loss can be approximated as

$$\begin{aligned}\ell_b(\mathbf{w}_b, \mathbf{z}_{b-1}^k) &\approx \ell_b(\mathbf{w}_b^k, \mathbf{z}_{b-1}^k) + \left\langle \frac{\partial \ell_b}{\partial \mathbf{w}_b^k}, \mathbf{w}_b - \mathbf{w}_b^k \right\rangle + \frac{1}{2}(\mathbf{w}_b - \mathbf{w}_b^k)^T \mathbf{H}_W (\mathbf{w}_b - \mathbf{w}_b^k) \\ &\approx \ell_b(\mathbf{w}_b^k, \mathbf{z}_{b-1}^k) + \left\langle \frac{\partial \ell_b}{\partial \mathbf{w}_b^k}, \mathbf{w}_b - \mathbf{w}_b^k \right\rangle + \frac{1}{2}m_{b,W}\|\mathbf{w}_b - \mathbf{w}_b^k\|_2^2,\end{aligned}\quad (20)$$

$$\ell_b(\mathbf{w}_b^k, \mathbf{z}_{b-1}) \approx \ell_b(\mathbf{w}_b^k, \mathbf{z}_{b-1}^k) + \left\langle \frac{\partial \ell_b}{\partial \mathbf{z}_{b-1}^k}, \mathbf{z}_{b-1} - \mathbf{z}_{b-1}^k \right\rangle + \frac{1}{2}m_{b,z}\|\mathbf{z}_{b-1} - \mathbf{z}_{b-1}^k\|_2^2,\quad (21)$$

where the approximation is composed of a second-order Taylor expansion and a scaling effect of local Hessian, and  $\mathbf{w}_b$  may represent  $\text{vec}(\mathbf{W}_b)$  contingent on the context.

We next propose an algorithm *scale-amended SGD* to take the effect of  $m_{b,W}$  and  $m_{b,z}$  into account to balance the training pace of each block. *Scale-amended SGD* uses  $m_{b,W}$  and  $m_{b,z}$  to amend the scale of vanilla BP of each block. We set the initial *backward factor* of the output layer  $m = 1$ , which indicates that the derivative of the loss with respect to the output of the network is regarded as the desired changes on the output to minimize the loss.

Then following the backward order, if a block has parameter  $\mathbf{W}_b$  and gradient  $\delta\mathbf{W}_b$  computed by BP, then we use  $\delta'\mathbf{W}_b := \delta\mathbf{W}_b/m/m_{b,W}$  as the scale-amended gradient to update  $\mathbf{W}_b$ , where  $m$  is the backward factor on the output of the block and  $m_{b,W}$  is the scalar used to approximate  $\mathbf{H}_{b,W}$ . Then we update the backward factor  $m$  for next block via  $m \leftarrow m \cdot m_{b,z}$ , where  $m_{b,z}$  is the scalar used to approximate  $\mathbf{H}_{b,z}$ . This strategy is described in Algorithm 2.

### 4.1 Scale-amended SGD for feed-forward networks with BN

Note that for the feed-forward networks with BN layers, we can obtain a reliable estimation of  $m_{b,W}$  and  $m_{b,z}$ . Specifically, we assume that  $\mathbf{W}_b$  is row homogeneous [Ba et al., 2016], i.e., they represent the same level of information and are roughly of similar magnitude, and define

$$\|\mathbf{W}_b\|_{2,\mu}^2 := \frac{1}{\#\text{row}(\mathbf{W}_b)} \sum_{i=1}^{\#\text{row}(\mathbf{W}_b)} \mathbf{w}_b(i)^T \mathbf{w}_b(i),$$

---

**Algorithm 2** Scale-amended SGD

---

**Input:** Gradient  $\delta \mathbf{W}_b$  and scaling factor  $m_{b,W}, m_{b,z}$ . **for**  $b = 1, \dots, B$ ; **Initialize**  $m = 1$ .

**for**  $b = B, \dots, 1$  **do**

$$\delta' \mathbf{W}_b \leftarrow \delta \mathbf{W}_b / m / m_{b,W} \quad (22)$$

$$m \leftarrow m \cdot m_{b,z} \quad (23)$$

**end for**

---

where  $w_b(i)$  is the  $i$ -th row of  $\mathbf{W}_b$ . Under this assumption, the scalars to approximate the local Hessians (17) and (18) of the fully connected layer with BN are computed as follows,

$$m_{b,z} := \|\mathbf{W}_b^T\|_{2,\mu}^2 / \|\mathbf{W}_b\|_{2,\mu}^2, \quad m_{b,W} := 1 / \|\mathbf{W}_b\|_{2,\mu}^2. \quad (24)$$

We next evaluate the *scale-amended SGD* on training VGG nets [Simonyan and Zisserman, 2015] for image classification tasks with two datasets: CIFAR-10 [Krizhevsky and Hinton, 2009] and CIFAR-100 [Krizhevsky and Hinton, 2009]. We modify the VGG nets by keeping the last fully connected layers and removing the intermediate two fully connected layers and all the biases. Each intermediate layer of the VGG nets concatenates a BN layer right before the activation function and the BN has no trainable parameters.

During training, the images of CIFAR-10 and CIFAR-100 datasets are randomly flipped and rotated for data augmentation. The hyper-parameters for vanilla SGD and our scale-amended SGD are the same including learning rate  $\eta = 0.1$  (because the backward factor for linear layer of CIFAR10 is around  $\frac{10}{512}$ , small learning rate  $\eta = 0.005$  works better for CIFAR10 to use scale-amended SGD), momentum 0.9 and weight decay<sup>5</sup> coefficient 0.005. We reduce the learning rate by half once the validation accuracy is on plateau (ReduceLROnPlateau in PyTorch with patience=10), which works well for both vanilla-SGD and scale-amended SGD.

We compare the learning curves between *scale-amended SGD* and vanilla SGD on training VGG13 for CIFAR10 and CIFAR-100 classification tasks. Two algorithms start from the same initialization and pass the same batches of data. Both algorithms are run 300 epochs. We plot the learning curves in Figure 1. From Figure 1, we can see that the learning curves of our algorithm and SGD have

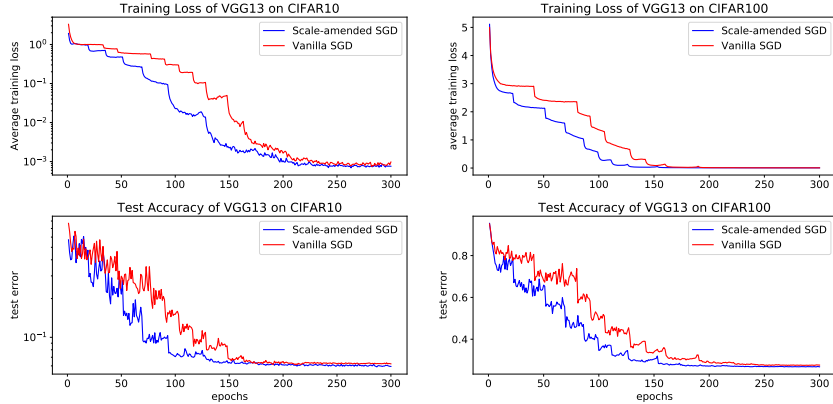


Figure 1: Comparison of vanilla SGD and *scale-amended SGD* on training VGG13 for CIFAR10 and CIFAR-100 classification. Hyperparameters are the same: learning rate 0.1 (except for CIFAR10 scale-amended SGD uses 0.005), momentum 0.9, weight decay 0.005.

similar trend (we plot curves of multiple runs and their average in Supplemental D). This is because *scale-amended SGD* only modifies the magnitude of each block gradient as a whole and does not involve any further information (second order information) and hyper-parameters are the same for both algorithms. Scrutinizing more closely, we can see our training loss curve is almost always lower than SGD’s and our test error ends with a considerably lower number. Thus the scale-amended SGD

---

<sup>5</sup>For *scale-amended SGD*, we first apply the weight decay and then amend the scale.



achieves favorable result over vanilla SGD on training feed-forward neural network with BN. More extensive experiments can be found in Supplemental D.

## 5 Conclusion

In this paper we view BP as a solution of *back-matching propagation* which minimizes a sequence of back-matching losses. By studying the Hessian of the local back-matching loss, we interpret the benefits of practical designing tricks, e.g., batch normalization and skip connection, in a unified way: improving the spectrum of local Hessian. Moreover, we propose scale-amended SGD algorithm by employing the information of local Hessian via a scalar approximation. Scale-amended SGD achieves favorable results over vanilla SGD empirically for training feed-forward networks with BN, which corroborates the importance of local Hessian.

## Acknowledgments

The authors would like to thank Prof. Yuejie Chi for helpful discussion.

## References

- M. Abadi, P. Barham, J. Chen, Z. Chen, A. Davis, J. Dean, M. Devin, S. Ghemawat, G. Irving, M. Isard, et al. TensorFlow: A system for large-scale machine learning. In *OSDI*, volume 16, pages 265–283, 2016.
- S.-I. Amari. Natural gradient works efficiently in learning. *Neural computation*, 10(2):251–276, 1998.
- J. L. Ba, J. R. Kiros, and G. E. Hinton. Layer normalization. *arXiv preprint arXiv:1607.06450*, 2016.
- F. Bastien, P. Lamblin, R. Pascanu, J. Bergstra, I. Goodfellow, A. Bergeron, N. Bouchard, D. Warde-Farley, and Y. Bengio. Theano: new features and speed improvements. *arXiv preprint arXiv:1211.5590*, 2012.
- A. Ben-Tal and A. Nemirovski. *Lectures on modern convex optimization: analysis, algorithms, and engineering applications*, volume 2. Siam, 2001.
- M. Carreira-Perpinan and W. Wang. Distributed optimization of deeply nested systems. In *Artificial Intelligence and Statistics*, pages 10–19, 2014.
- P. Chen. Hessian matrix vs. Gauss–Newton matrix. *SIAM Journal on Numerical Analysis*, 49(4):1417–1435, 2011.
- M. Cho and J. Lee. Riemannian approach to batch normalization. In *Advances in Neural Information Processing Systems (NIPS)*, pages 5231–5241, 2017.
- Y. N. Dauphin, R. Pascanu, C. Gulcehre, K. Cho, S. Ganguli, and Y. Bengio. Identifying and attacking the saddle point problem in high-dimensional non-convex optimization. In *Advances in Neural Information Processing Systems (NIPS)*, pages 2933–2941, 2014.
- T. Frerix, T. Möllenhoff, M. Moeller, and D. Cremers. Proximal backpropagation. In *International Conference on Learning Representations (ICLR)*, 2018.
- R. Grosse and J. Martens. A Kronecker-factored approximate Fisher matrix for convolution layers. In *International Conference on Machine Learning (ICML)*, 2016.
- K. He, X. Zhang, S. Ren, and J. Sun. Deep residual learning for image recognition. In *The IEEE Conference on Computer Vision and Pattern Recognition (CVPR)*, June 2016a.
- K. He, X. Zhang, S. Ren, and J. Sun. Identity mappings in deep residual networks. In *European Conference on Computer Vision*, pages 630–645. Springer, 2016b.
- G. Hinton, L. Deng, D. Yu, G. E. Dahl, A.-r. Mohamed, N. Jaitly, A. Senior, V. Vanhoucke, P. Nguyen, T. N. Sainath, et al. Deep neural networks for acoustic modeling in speech recognition: The shared views of four research groups. *IEEE Signal Processing Magazine*, 29(6):82–97, 2012.
- S. Hochreiter. Untersuchungen zu dynamischen neuronalen netzen. *Diploma, Technische Universität München*, 1991.
- S. Hochreiter and J. Schmidhuber. Long short-term memory. *Neural Computation*, 9(8):1735–1780, 1997.

- S. Hochreiter, Y. Bengio, P. Frasconi, J. Schmidhuber, et al. Gradient flow in recurrent nets: the difficulty of learning long-term dependencies, 2001.
- G. Huang, Z. Liu, K. Q. Weinberger, and L. van der Maaten. Densely connected convolutional networks. In *The IEEE Conference on Computer Vision and Pattern Recognition (CVPR)*, volume 1, page 3, 2017a.
- L. Huang, X. Liu, B. Lang, and B. Li. Projection based weight normalization for deep neural networks. *arXiv preprint arXiv:1710.02338*, 2017b.
- S. Ioffe and C. Szegedy. Batch normalization: Accelerating deep network training by reducing internal covariate shift. In *International Conference on Machine Learning (ICML)*, pages 448–456, 2015.
- S. Jastrzebski, D. Arpit, N. Ballas, V. Verma, T. Che, and Y. Bengio. Residual connections encourage iterative inference. In *International Conference on Learning Representations (ICLR)*, 2018.
- S. Jastrzebski, Z. Kenton, N. Ballas, A. Fischer, A. Storkey, and Y. Bengio. SGD smooths the sharpest directions. 2018.
- A. Krizhevsky and G. Hinton. Learning multiple layers of features from tiny images. 2009.
- J. Lafond, N. Vasilache, and L. Bottou. Diagonal rescaling for neural networks. *arXiv preprint arXiv:1705.09319*, 2017.
- Y. Le Cun. Learning process in an asymmetric threshold network. In *Disordered systems and biological organization*, pages 233–240. Springer, 1986.
- Y. Le Cun, I. Kanter, and S. A. Solla. Eigenvalues of covariance matrices: Application to neural-network learning. *Physical Review Letters*, 66(18):2396, 1991.
- D.-H. Lee, S. Zhang, A. Fischer, and Y. Bengio. Difference target propagation. In *Joint European Conference on Machine Learning and Knowledge Discovery in Databases*, pages 498–515. Springer, 2015.
- S. Li, J. Jiao, Y. Han, and T. Weissman. Demystifying resnet. *arXiv preprint arXiv:1611.01186*, 2016.
- V. A. Marčenko and L. A. Pastur. Distribution of eigenvalues for some sets of random matrices. *Mathematics of the USSR-Sbornik*, 1(4):457, 1967.
- J. Martens. Deep learning via Hessian-free optimization. In *International Conference on Machine Learning (ICML)*, pages 735–742, 2010.
- J. Martens. *Second-order optimization for neural networks*. PhD thesis, University of Toronto, 2016.
- J. Martens and R. Grosse. Optimizing neural networks with Kronecker-factored approximate curvature. In *International Conference on Machine Learning (ICML)*, pages 2408–2417, 2015.
- D. Mishkin and J. Matas. All you need is a good init. In *International Conference on Learning Representations (ICLR)*, 2016.
- J. Nocedal and S. J. Wright. *Sequential quadratic programming*. Springer, 2006.
- Y. Ollivier. Riemannian metrics for neural networks I: feedforward networks. *Information and Inference: A Journal of the IMA*, 4(2):108–153, 2015.
- A. E. Orhan and X. Pitkow. Skip connections eliminate singularities. In *International Conference on Learning Representations (ICLR)*, 2018.
- R. Pascanu and Y. Bengio. Revisiting natural gradient for deep networks. In *International Conference on Learning Representations (ICLR)*, 2014.
- A. Paszke, S. Gross, S. Chintala, G. Chanan, E. Yang, Z. DeVito, Z. Lin, A. Desmaison, L. Antiga, and A. Lerer. Automatic differentiation in PyTorch. 2017.
- D. E. Rumelhart, G. E. Hinton, and R. J. Williams. Learning representations by back-propagating errors. *Nature*, 323(6088):533, 1986.
- L. Sagun, U. Evci, V. U. Guney, Y. Dauphin, and L. Bottou. Empirical analysis of the hessian of over-parametrized neural networks. *arXiv preprint arXiv:1706.04454*, 2017.
- A. Saxe, J. L. McClelland, and S. Ganguli. Exact solutions to the nonlinear dynamics of learning in deep linear neural networks. In *International Conference on Learning Representations (ICLR)*, 2014.

- F. Seide and A. Agarwal. CNTK: Microsoft’s open-source deep-learning toolkit. In *Proceedings of the 22nd ACM SIGKDD International Conference on Knowledge Discovery and Data Mining*, pages 2135–2135. ACM, 2016.
- K. Simonyan and A. Zisserman. Very deep convolutional networks for large-scale image recognition. In *International Conference on Learning Representations (ICLR)*, 2015.
- B. Singh, S. De, Y. Zhang, T. Goldstein, and G. Taylor. Layer-specific adaptive learning rates for deep networks. In *IEEE 14th International Conference on Machine Learning and Applications (ICMLA)*, pages 364–368, Dec 2015.
- A. Veit, M. J. Wilber, and S. Belongie. Residual networks behave like ensembles of relatively shallow networks. In *Advances in Neural Information Processing Systems (NIPS)*, pages 550–558, 2016.
- S. Wiseman, S. Chopra, M. Ranzato, A. Szlam, R. Sun, S. Chintala, and N. Vasilache. Training language models using target-propagation. *arXiv preprint arXiv:1702.04770*, 2017.
- C. Ye, Y. Yang, C. Fermuller, and Y. Aloimonos. On the importance of consistency in training deep neural networks. *arXiv preprint arXiv:1708.00631*, 2017.
- Y. You, I. Gitman, and B. Ginsburg. Large batch training of convolutional networks. *arXiv preprint arXiv:1708.03888v3*, 2017.
- H. Zhang, C. Xiong, J. Bradbury, and R. Socher. Block-diagonal hessian-free optimization for training neural networks. *arXiv preprint arXiv:1712.07296*, 2017.
- B. Zoph and Q. V. Le. Neural architecture search with reinforcement learning, 2016.

## Supplementary Material

### A Proof for Proposition 1

The proof is straightforward. The key is to show the one-step gradient update of

$$\mathbf{z}_{b-1}^{k+\frac{1}{2}} \leftarrow \arg \min_{\mathbf{z}_{b-1}} \ell_b(\mathbf{W}_b^k, \mathbf{z}_{b-1}) \quad (25)$$

with step size 1 satisfies

$$\mathbf{z}_{b-1}^{k+\frac{1}{2}} - \mathbf{z}_{b-1}^k = - \frac{\partial J}{\partial \mathbf{z}_{b-1}} \Big|_{\mathbf{W}=\mathbf{W}^k, \mathbf{z}=\mathbf{z}^k}, \quad (26)$$

where  $J$  is given by Equation 1.

For the case  $b = B$ , we have  $\ell_b(\mathbf{W}_b, \mathbf{z}_{b-1}) = \ell(\mathbf{y}^k; F_B(\mathbf{W}_B, \mathbf{z}_{B-1}))$ , and the one-step gradient solution of (25) is

$$\mathbf{z}_{B-1}^{k+\frac{1}{2}} = \mathbf{z}_{B-1}^k - 1 \cdot \frac{\partial \ell_B}{\partial \mathbf{z}_{B-1}} \Big|_{\mathbf{W}_B=\mathbf{W}_B^k, \mathbf{z}_{B-1}=\mathbf{z}_{B-1}^k}, \quad (27)$$

which satisfies (26).

For other cases of  $b$ , we have  $\ell_b(\mathbf{W}_b, \mathbf{z}_{b-1}) = \frac{1}{2} \left\| \mathbf{z}_b^{k+\frac{1}{2}} - F_b(\mathbf{W}_b, \mathbf{z}_{b-1}) \right\|^2$ . Suppose the one-step gradient solution of (25) satisfies (26) for some  $b$ . We next verify it for the case  $b-1$ . Since

$$\mathbf{z}_{b-2}^{k+\frac{1}{2}} = \mathbf{z}_{b-2}^k - 1 \cdot \frac{\partial \ell_{b-1}}{\partial \mathbf{z}_{b-2}} \Big|_{\mathbf{W}_{b-1}=\mathbf{W}_{b-1}^k, \mathbf{z}_{b-2}=\mathbf{z}_{b-2}^k}, \quad (28)$$

then

$$\begin{aligned} \mathbf{z}_{b-2}^{k+\frac{1}{2}} - \mathbf{z}_{b-2}^k &= - \frac{\partial \ell_{b-1}}{\partial \mathbf{z}_{b-2}} \Big|_{\mathbf{W}_{b-1}=\mathbf{W}_{b-1}^k, \mathbf{z}_{b-2}=\mathbf{z}_{b-2}^k} \\ &= \left( \frac{\partial F_{b-1}}{\partial \mathbf{z}_{b-2}} \Big|_{\mathbf{W}_{b-1}=\mathbf{W}_{b-1}^k, \mathbf{z}_{b-2}=\mathbf{z}_{b-2}^k} \right)^T \cdot (\mathbf{z}_{b-1}^{k+\frac{1}{2}} - \mathbf{z}_{b-1}^k) \\ &= - \left( \frac{\partial F_{b-1}}{\partial \mathbf{z}_{b-2}} \cdot \frac{\partial J}{\partial \mathbf{z}_{b-1}} \right) \Big|_{\mathbf{W}=\mathbf{W}^k, \mathbf{z}=\mathbf{z}^k} \end{aligned} \quad (29)$$

$$= - \frac{\partial J}{\partial \mathbf{z}_{b-2}} \Big|_{\mathbf{W}=\mathbf{W}^k, \mathbf{z}=\mathbf{z}^k}. \quad (30)$$

Following chain rule, this completes the proof.

### B BP through BN for back-matching loss

The gradient for the back matching loss of a fully connected layer with BN is given by

$$\frac{\partial \ell_b}{\partial \mathbf{z}_b} = \mathbf{z}_b - \mathbf{z}_b^{k+\frac{1}{2}}, \quad (31)$$

$$\frac{\partial \ell_b}{\partial \tilde{\mathbf{z}}_b} = \frac{\partial \ell_b}{\partial \mathbf{z}_b} \cdot \frac{1}{\sqrt{\text{Var}[\tilde{\mathbf{z}}_b]}} + \frac{\partial \ell_b}{\partial \text{Var}[\tilde{\mathbf{z}}_b]} \cdot \frac{2(\tilde{\mathbf{z}}_b - \mathbb{E}[\tilde{\mathbf{z}}_b])}{m} + \frac{1}{m} \cdot \frac{\partial \ell_b}{\partial \mathbb{E}[\tilde{\mathbf{z}}_b]}, \quad (32)$$

$$\frac{\partial \ell_b}{\partial \mathbf{z}_{b-1}} = (\mathbf{W}_b^k)^T \frac{\partial \ell_b}{\partial \tilde{\mathbf{z}}_b}, \quad (33)$$

$$\frac{\partial \ell_b}{\partial \mathbf{w}_b} = \frac{\partial \ell_b}{\partial \tilde{\mathbf{z}}_b} \cdot (\mathbf{z}_{b-1}^k)^T, \quad (34)$$

where  $m$  is the mini-batch size, and  $\frac{\partial \ell_b}{\partial \text{Var}[\tilde{\mathbf{z}}_b]}$  and  $\frac{\partial \ell_b}{\partial \mathbb{E}[\tilde{\mathbf{z}}_b]}$  is the gradient on quantities  $\text{Var}[\tilde{\mathbf{z}}_b]$  and  $\mathbb{E}[\tilde{\mathbf{z}}_b]$  respectively.

### C Local Hessian for convolutional layer

In this part we derive the Hessian of the back-matching loss for a convolutional layer. We change the notation a bit for clear representation. The weight parameter  $\mathbf{W}$  is an array with dimension  $n \times m \times w \times h$ , where  $n$  and  $m$  are the number of output features and the number of input features respectively, and  $w$  and  $h$  are the

width and height of convolutional kernels. Suppose the output feature size is  $q_1 \times q_2$  and the input feature size is  $p_1 \times p_2$ . We use  $b_{ku_1u_2}$  to denote the output at location  $(u_1, u_2)$  of feature  $k$  and  $a_{ju_1u_2}$  to denote the input at location  $(u_1, u_2)$  of feature  $j$ , then the forward process is

$$b_{ku_1u_2} = \sum_{j=1}^n \sum_{v_1v_2} a_{j(u_1+v_1)(u_2+v_2)} w_{jkv_1v_2}, \quad (35)$$

and the BP is given by

$$\delta a_{ju_1u_2} = \sum_{k=1}^m \sum_{v_1v_2} \delta b_{k(u_1+v_1)(u_2+v_2)} w_{jkv_1v_2}, \quad (36)$$

$$\delta w_{jkv_1v_2} = \sum_{u_1u_2} \delta b_{ku_1u_2} a_{j(u_1+v_1)(u_2+v_2)}. \quad (37)$$

However, this formula of the forward and backward process of convolutional layer make the derivation of Hessian complex. Note that the convolution operation essentially performs dot products between the convolution kernels and local regions of the input. The forward pass of a convolution layer can be formulated as one big matrix multiply with *im2col* operation. In order to describe back matching process clearly, we rewrite the convolution layer forward and backward pass with *im2col* operation. We use  $\mathbf{W}_{row}$  and  $\mathbf{W}_{col}$  to represent the weight matrices with dimension  $n \times (mwh)$  and  $m \times (nwh)$ , respectively, which both are stretched out from  $\mathbf{W}(n, m, w, h)$ . To mimic the convolutional operation, we rearrange the input features  $\mathbf{a}$  into a big matrix  $\mathbf{a}_{i2c}$  through *im2col* operation: each column of  $\mathbf{z}_{i2c}$  is composed of the elements of  $\mathbf{a}$  that are used to compute one location in  $\mathbf{b}$ . Thus if  $\mathbf{b}$  has dimension  $n \times q_1 \times q_2$ , then  $\mathbf{a}_{i2c}$  has dimension  $mwh \times q_1q_2$ . Furthermore, we stack the latter two dimensions of  $\mathbf{b}$  into a tall vector, denoted as  $\mathbf{b}_{col}$  which has dimension  $n \times q_1q_2$ . The forward process (35) of convolutional layer can be rewritten as

$$\mathbf{b}_{col} = \mathbf{W}_{row} \mathbf{a}_{i2c} \quad (38)$$

Similarly, we can rewrite the regular BP (36) and (37) as

$$\delta a_{ju_1u_2}(x) = \mathbf{w}_{ju_1u_2 \rightarrow}^T \delta \mathbf{b}(x), \quad (39)$$

$$\delta \mathbf{W}_{row} = \mathbb{E}_x \delta \mathbf{b}_{col}(x) \mathbf{z}_{i2c}^T(x), \quad (40)$$

where  $\mathbf{w}_{ju_1u_2 \rightarrow}$  is a vector of dimension  $nq_1q_2$ , whose non-zero elements are those weights that interact with input location  $ju_1u_2$ . There are approximately  $n \times wh/c$  non-zero elements and  $c$  is a factor related with pooling, padding and stride (if padding=same-size, stride=2, then  $c=4$ ). The non-zero elements are scattered into  $n$  blocks, with each block  $wh/c$  non-zero elements, whose location within the block is corresponding to  $(u_1, u_2)$ . With these notations, we can derive the formula of local Hessian, given by

$$\mathbf{H}_{W_n} = \mathbb{E} \mathbf{a}_{i2c} \mathbf{a}_{i2c}^T, \quad (41)$$

$$\mathbf{H}_a(j, u_1, u_2, k, v_1, v_2) = \frac{\partial^2 \ell}{\partial a_{ju_1u_2} \partial a_{kv_1v_2}} = \mathbf{w}_{ju_1u_2 \rightarrow}^T \mathbf{w}_{kv_1v_2 \rightarrow}, \quad (42)$$

$$\mathbf{H}_a = \mathbf{W}_a^T \mathbf{W}_a, \quad (43)$$

where  $\mathbf{W}_a$  is a  $nq_1q_2 \times mp_1p_2$  matrix each column being  $\mathbf{w}_{ju_1u_2 \rightarrow}$ . We know  $\mathbf{W}_a$  is a sparse matrix and so is  $\mathbf{H}_a$ . Moreover,  $\mathbf{H}_{W_n}$  is a concentrated matrix as each component is a summation of  $q_1q_2 \times$  batch-size variables. As the convolutional layer is essentially a linear mapping, the formulas here is similar to those of the fully connected layer although they are more involved.

### C.1 Approximate convolution layer with BN

We approximate  $\mathbf{H}_{W_n}$  by a scalar  $m_{b,W_n} = s / \|\mathbf{W}_{row}\|_{2,\mu}^2$ , where  $s = q_1q_2$  is the sharing parameter and  $q_1 \times q_2$  is the output feature size.

We approximate  $\mathbf{H}_a$  by a scalar  $m_{b,z} = \|\mathbf{W}_{col}\|_{2,\mu}^2 / \|\mathbf{W}_{row}\|_{2,\mu}^2 / c$ , where  $c$  is a factor related with pooling, padding and stride (if padding=same-size, stride=2, then  $c=4$ ).

## D Other experiments

In order to verify the stability of scale-amended SGD, we run and plot multiple times of the learning curves as in Figure 1 here. We do extensive experiments to verify the effectivity of scale-amended SGD on training feed-forward neural networks with BN. First we introduce several baseline algorithms and their settings.

The first base algorithm is the vanilla SGD with *Nesterov momentum* 0.9. The learning rate is chosen to be  $\eta = 0.1$  given a pool of candidates  $\{0.01, 0.05, 0.1, 0.2, 0.5\}$ .

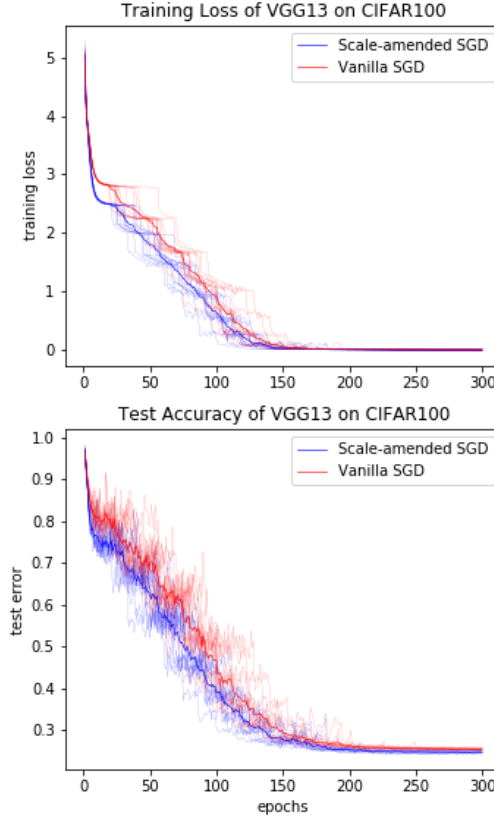


Figure 2: Multiple runs of Figure 1 for CIFAR100.

Table 1: Classification accuracies for CIFAR-10 and CIFAR-100.

	CIFAR10				CIFAR100			
	VGG11	VGG13	VGG16	VGG19	VGG11	VGG13	VGG16	VGG19
SGD	92.34	93.90	93.72	93.47	71.84	74.07	72.86	71.35
LARS	91.81	93.40	93.47	93.48	67.26	70.35	69.90	69.52
LSALR	92.58	93.68	93.35	93.46	71.14	73.74	73.14	70.76
OURS	92.45	<b>94.11</b>	<b>93.90</b>	<b>93.88</b>	<b>73.39</b>	<b>75.32</b>	<b>74.68</b>	<b>72.82</b>

The second baseline algorithm is LSALR which uses  $\eta \cdot (1 + \log(1 + 1/\|\delta \mathbf{W}_l\|_2))$  as the learning rate for the layer  $l$ . The global learning rate is set to be  $\eta = 0.1$ , which achieves best performance comparing from a pool of candidates  $\{0.006, 0.05, 0.1, 0.2, 0.5\}$ .

The third baseline algorithm is LARS which uses  $\eta \cdot \frac{\|\mathbf{W}_l\|_2}{\|\delta \mathbf{W}_l\|_2}$  as the learning rate for layer  $l$ . In our experiment, we use the global learning rate  $\eta = 2$  for LARS, which achieves best performance from a pool of  $\{0.1, 1, 2, 5, 10\}$ .

For baseline algorithms, we apply *weight decay* with coefficient  $1e-3$  if without specific description.

At last, we present the test accuracy of different VGG nets for classification of CIFAR-10 and CIFAR-100 in Table 1. We report the median of 3 independent runs of each pair of model and algorithm. For this group of experiments, we use global learning rate  $\eta = 0.1$  and weight decay coefficient  $5e-3$  for our algorithm. Our algorithm achieves higher test accuracy over its competitors on all four VGG models with margins.